Near-zero volume-shrinkage in reactive sintering of porous MgTi₂O₅ with pseudobrookite-type structure

Yuta NAKAGOSHI[a], Jun SATO[b], Masahumi MORIMOTO[b], and Yoshikazu SUZUKI[a,c*]

[a] Graduate School of Pure and Applied Sciences, University of Tsukuba, 1-1-1 Tennodai, Tsukuba, Ibaraki, 305-8573, Japan

[b] Quantachrome Instruments Japan G.K., KSP W311, 3-2-1 Sakado Takatsu, Kawasaki, Kanagawa 213-0012, Japan

[c] Faculty of Pure and Applied Sciences, University of Tsukuba, 1-1-1 Tennodai, Tsukuba, Ibaraki, 305-8573, Japan

Abstract

Reactive sintering is an environmentally-friendly processing for porous ceramics. If zero volume-shrinkage in the reactive sintering is realized, the reactive sintering will be more widely applied. Here, we report a new reactive sintering technique to realize near-zero volume-shrinkage (NZVS) in the MgO-TiO$_2$ system. Porous MgTi$_2$O$_5$ pellets have been reactively sintered from LiF-doped hydromagnesite/TiO$_2$ mixed powders with changing TiO$_2$ anatase/rutile compositions. By using the anatase and rutile mixtures as TiO$_2$ source, volume-shrinkage during the sintering was well-controlled. In particular, the NZVS is realized for the sintering temperatures at 1000‑1100°C. To clarify the mechanism of the NZVS phenomenon, MgTi$_2$O$_5$ particle formation behavior from the identical starting powders without pelletizing was investigated in detail. From the microstructural observation for MgTi$_2$O$_5$ powders, TiO$_2$ rutile prevented the crystal growth of MgTi$_2$O$_5$ particles.

Keywords: A. Powders: solid state reaction; A. Shaping; A. Sintering; B. Porosity; Magnesium dititanate (MgTi$_2$O$_5$); Pore-size distribution

1. Introduction

Porous ceramics have been applied for various fields with development in ceramic engineering, in particular, for refractory materials. In recent years, environmental and energy issues have attracted more and more interest. Therefore, considerable attentions have been directed toward the applications of porous ceramics for environmental and/or energy devices,

---

* Corresponding author:
Division of Materials Science, Faculty of Pure and Applied Sciences,
University of Tsukuba, Ibaraki 305-8573, Japan
E-mail: suzuki@ims.tsukuba.ac.jp

e.g. various purification filters and fuel cells. Magnesium dititanate ($MgTi_2O_5$), with orthorhombic pseudobrookite-type structure, has a negative or very small thermal expansion in one axis, *i.e. a*-axis in the space group *Cmcm* (or *c*-axis in the space group *Bbmm*) [1-3]. This strong thermal expansion anisotropy induces the formation of intergranular and intragranular microcracks. These microcracks relax the thermal stress of particles; hence, the pseudobrookite-type ceramics have low coefficients of bulk thermal expansion [4-5]. $MgTi_2O_5$ is thermally stable among various pseudobrookite-type ceramics [6-9], and also, it is low-cost and non-toxic. With these notable properties, $MgTi_2O_5$ has a high potential as a thermal-shock resistant material.

To date, porous ceramics have been prepared by various processes [10-11]; reactive sintering is an environmentally-friendly process because it does not need any pore forming agents [12-16]. Suzuki *et al.* reported the synthesis of porous $MgTi_2O_5$ by the reactive sintering from hydromagnesite ($Mg_5(CO_3)_4(OH)_2 \cdot 4H_2O$) and TiO_2 anatase mixed powder with lithium fluoride (LiF) additive [17-19]. However, the decomposition of hydromagnesite in the reactive sintering resulted in some volume shrinkage of samples. If zero volume-shrinkage (or more favorably near-net shaping) in the reactive sintering is realized, the reactive sintering will be more widely applied.

Here, we report a new reactive sintering technique to realize near-zero volume-shrinkage (NZVS) in the MgO-TiO_2 system. Porous $MgTi_2O_5$ pellets have been reactively sintered from LiF-doped hydromagnesite/TiO_2 mixed powders with changing TiO_2 anatase/rutile compositions. By using the anatase and rutile mixtures as TiO_2 source, volume-shrinkage during the sintering was well-controlled. The pore-size distributions of porous $MgTi_2O_5$ pellets were measured by mercury intrusion porosimetry. To clarify the mechanism of the NZVS phenomenon, $MgTi_2O_5$ particle formation behavior from the identical starting powders without pelletizing was investigated in detail, including *in situ* high-temperature X-ray diffraction for reaction analysis, and microstructural observation of $MgTi_2O_5$ particles.

2. Experimental procedures

2.1. Preparation and characterization of bulk porous $MgTi_2O_5$ using TiO_2 anatase/rutile mixture

Commercially available hydromagnesite ($Mg_5(CO_3)_4(OH)_2 \cdot 4H_2O$) powder, TiO_2 anatase powder and TiO_2 rutile powder (99.9% purity each, Kojundo Chemical Laboratory Co. Ltd.) were used as the starting materials. In this study, the following TiO_2 anatase/rutile compositions (in mole fraction) were used: (a) anatase : rutile = 100 : 0, (b) 75 : 25, (c) 50 : 50, (d) 25 : 75 and (e) 0 : 100. LiF powder (98.0%, Wako Pure Chemical, Osaka, Japan) was used as a mineralizer. Prior to the weighing, TG-DTA analysis (up to 1000°C) on each starting powder was conducted to determine the weight-loss during the heating. With the compositional calibration using

TG-DTA results, hydromagnesite and TiO_2 powders (Mg:Ti = 1:2 in mole fraction) with LiF (0.5 wt.% for total starting powders) were wet-ball milled in ethanol for 24 h. The mixed slurries were vacuum dried, and the dried powders were put into the oven at 80°C overnight. The mixed powders, with a variety of TiO_2 anatase/rutile compositions (a)-(e), were then sieved through a 150-mesh screen. All mixed powders had almost the same average particle-sizes. (See supporting information **Fig. S1** and Table S1 on the particle-size distribution after sieving.)

The five mixed powders (4.0 g each) were uniaxially pressed at 16.6 MPa for 1 min to obtain green compacts with a diameter of 15 mm and a thickness of ~4 mm. The green compacts were sintered at 1000-1200°C in air for 2 h to obtain porous $MgTi_2O_5$ pellets. The volume of the pellets was measured before and after reactive sintering, in order to examine their volume changes. The microstructure of the porous $MgTi_2O_5$ pellets sintered at 1100°C was observed by scanning electron microscopy (SEM, JSM-5600, JEOL, Tokyo, Japan). The pore-size distribution was measured by mercury intrusion porosimetry (Poremaster, Quantachrome Instruments).

2.2. Effect of TiO_2 anatase/rutile composition on $MgTi_2O_5$ particle formation behavior

To clarify the mechanism of the NZVS phenomenon, $MgTi_2O_5$ particle formation behavior from the starting powders, with a variety of TiO_2 anatase/rutile compositions (a)-(e), was investigated. The mixed powders were calcined (without pelletizing) at 1100°C in air for 2 h to obtain the $MgTi_2O_5$ powders.

The constituent phases of $MgTi_2O_5$ powders were analyzed by X-ray diffraction method (XRD, Cu-K$_\alpha$, 40 kV and 40 mA, Multiflex, Rigaku, Tokyo, Japan). The microstructure of the $MgTi_2O_5$ powders was observed by SEM. The reaction behavior of the mixed powders (a) and (e) (i.e., 100% anatase and 100% rutile as a TiO_2 source, respectively) were analyzed by high-temperature X-ray diffraction (HT-XRD) in the range between room temperature and 1100°C in air. Each XRD pattern was acquired after 5 min holding at each temperature.

3. Results and discussion

3.1. Volume-shrinkage control in reactive sintering of porous $MgTi_2O_5$

Figure 1 demonstrates the appearances of porous $MgTi_2O_5$ pellets sintered at 1000−1200°C from the mixed powders with different TiO_2 anatase/rutile compositions. The differences of volume shrinkage were clearly observed through horizontal (sintering temperature) and vertical (anatase/rutile composition) axes. All pellets were composed of substantially single-phase $MgTi_2O_5$, confirmed by XRD analysis (not shown).

Figure 2, quantified from Fig. 1, shows the volume change of porous $MgTi_2O_5$ pellets with sintering temperature. Only the pellets prepared from the mixed powder with composition

(e) expanded after the reactive sintering at 1000,1050 and 1100°C. Such volume expansions can be attributed to the less sinterability and the less unit volume of TiO_2 rutile phase than TiO_2 anatase phase. For all compositions, the green compacts first expanded due to the decomposed CO_2 gas from hydromagnesite at about 500°C, and then shrank with increasing sintering temperature. For the composition (e), after the initial expansion, the volume shrinkage became minimized thanks to the less sinterability of TiO_2 rutile phase. As a result, the volume of pellets after the sintering at 1000,1050 and 1100°C became slightly larger than the green compact. Also, as can be seen from all five curves, the volume shrinkage can be controlled by changing the anatase/rutile compositions.

Figure 3, also quantified from Fig. 1, shows the volume change of porous $MgTi_2O_5$ pellets with TiO_2 anatase/rutile composition in the mixed powders. The volume change was almost proportional to the composition ratio of TiO_2 rutile phase. Hence, from Figs. 2 and 3, the zero volume-shrinkage in reactive sintering must be possible, specifically sintered at around 1000‑1150°C for the rutile composition of ~85-100%.

3.2. Pore-structure and microstructure of porous $MgTi_2O_5$ pellets

Figure 4 and **Table 1** show the pore-size distributions and quantified pore-structures of $MgTi_2O_5$ pellets sintered at 1100°C by using mixed powders with various TiO_2 anatase/rutile compositions, respectively. All of the porous $MgTi_2O_5$ pellets had very narrow pore-size distribution with a diameter of ~1 μm. With increasing rutile composition, the total pore volume (V_p) increased, and also the pore-size distribution sifted toward larger size, which was in good agreement with Section 3.1 (i.e., less sinterability of rutile-rich compositions).

Figure 5 demonstrates SEM micrographs of porous $MgTi_2O_5$ pellets sintered at 1100°C by using mixed powders with various TiO_2 anatase/rutile compositions. All pellets had complexly 3-D network structure, similarly to our previous works [18,19]. The $MgTi_2O_5$ pellets became more porous with increasing rutile composition. This result accorded with the pore structure studies by mercury intrusion porosimetry (Fig. 4).

3.3. Effect of TiO_2 anatase/rutile composition on $MgTi_2O_5$ particle formation behavior

In order to clarify the mechanism of the near-zero volume-shrinkage (NZVS) phenomenon, $MgTi_2O_5$ particle formation behavior was investigated using the identical starting powders in Section 3.1 without pelletizing. **Figure 6** shows XRD patterns for $MgTi_2O_5$ powders calcined at 1100°C by using LiF-doped hydromagnesite/TiO_2 mixed powders with various TiO_2 anatase/rutile compositions. Substantially single-phase $MgTi_2O_5$ powders were obtained from all raw powders; a trace amount of $MgTiO_3$, an intermediate phase of the MgO-TiO_2 reaction system, was found due to non-pelletizing.

Figure 7 shows high-temperature XRD patterns for the selected mixed powders: (a) the hydromagnesite and TiO_2 anatase, and (e) the hydromagnesite and TiO_2 rutile mixed powder both with 0.5 wt.% LiF. For these HT-XRD patterns, TiO_2 rutile does not affect the formation temperature of $MgTiO_3$ and $MgTi_2O_5$. The intermediate $MgTiO_3$ phase began to form around 800°C and the $MgTi_2O_5$ phase began to form around 1000°C by using both mixed powders. Consequently, the NZVS phenomenon observed in Section 3.1 cannot be attributed to the difference of reaction-phase development. This result supports the deduction that the NZVS phenomenon is presumably brought by the less sinterability and the less unit volume of TiO_2 rutile phase than TiO_2 anatase phase, as pointed out before.

Figure 8 demonstrates SEM micrographs of $MgTi_2O_5$ powders calcined (without pelletizing) at 1100°C by using the five mixed powders with various TiO_2 anatase/rutile compositions. Rod-like and coarse particles were obtained only in Fig. 8(a), i.e., by using only TiO_2 anatase as the starting material. This result agrees with our previous report, where rod-like $MgTi_2O_5$ particles were obtained from TiO_2 anatase with different LiF compositions [20]. In contrast, equi-axed and finer particles were obtained for TiO_2 rutile containing mixed powders (Fig. 8 (b‑e)). Hence, TiO_2 anatase in the starting powder accelerates the grain growth of $MgTi_2O_5$ (maybe also $MgTiO_3$), but TiO_2 rutile slows down the grain growth of $MgTi_2O_5$ (and maybe also $MgTiO_3$).

4. Conclusions

In this paper, a new reactive sintering technique to realize near-zero volume-shrinkage (NZVS) in the MgO-TiO_2 system was reported. In conclusions,

(1)   The volume shrinkage between before and after reactive sintering of porous $MgTi_2O_5$ pellets was successfully controlled by changing the composition of TiO_2 rutile phase in the mixed powders. The zero volume-shrinkage in reactive sintering must be possible, specifically sintered at around 1000‑1150°C for the rutile composition of ~85-100%.

(2)   With increasing rutile composition, the total pore volume (V_p) increased, and also the pore-size distribution sifted toward larger size, which was in good agreement with the macroscopic appearance change (Section 3.1) and microstructural observations (Section 3.2).

(3) TiO_2 anatase in the starting powder accelerates the grain growth of $MgTi_2O_5$ (maybe also $MgTiO_3$), but TiO_2 rutile slows down the grain growth of $MgTi_2O_5$ (and maybe also $MgTiO_3$).

The reactive sintering technique using anatase and rutile mixture, a key idea for NZVS, will be also promising for complicated near-net shaping in the future.

Acknowledgments

References

[1] G. Bayer, Thermal expansion characteristics and stability of pseudobrookite-type compounds, Me_3O_5. J. Less-Common Metals. 24 (1971) 129-138.

[2] J.J. Cleveland, R.C. Bradt, Grain size microcracking relations for pseudo-brookite oxides. J. Am. Ceram. Soc. 61 (1978) 478-481.

[3] D. Taylor, Thermal-expansion data .11. complex oxides, A_2BO_5, and the garnets. Br. Ceram. Trans. J. 86 (1987) 1-6.

[4] E.A. Bush, F.A. Hummel, High-temperature mechanical properties of ceramic materials .1. magnesium dititanate. J. Am. Ceram. Soc. 41 (1958) 189-195.

[5] J.A. Kuszyk, R.C. Bradt, Influence of grain-size on effects of thermal-expansion anisotropy in $MgTi_2O_5$. J. Am. Ceram. Soc. 56 (1973) 420-423.

[6] J. Hauck, crystallography and phase-relations of $MeO-M_2O_3-TiO_2$ systems (Me=Fe,Mg,Ni-M=Al,Cr,Fe). J. Solid State Chem. 36 (1981) 52-65.

[7] I. Shindo, Determination of the phase-diagram by the slow cooling float zone Method - the system $MgO-TiO_2$. J. Cryst. Growth. 50 (1980) 839-851.

[8] B.A. Wechsler, A. Navrotsky, Thermodynamics and structural chemistry of compounds in the system $MgO-TiO_2$. J. Solid State Chem. 55 (1984) 165-180.

[9] B.A. Wechsler, R.B. Vondreele, Structure refinements of Mg_2TiO_4, $MgTiO_3$ and $MgTi_2O_5$ by time-of-flight Neutron Powder Diffraction. Acta. Cryst. B. 45 (1989) 542-549.

[10] A.R. Studart, U.T. Gonzenbach, E. Tervoort, L.J. Gauckler, Processing routes to macroporous ceramics: A review. J. Am. Ceram. Soc. 89 (2006) 1771-1789.

[11] S. Deville, Freeze-casting of porous ceramics: A review of current achievements and issues. Adv. Eng. Mater. 10 (2008) 155-169.

[12] Y. Suzuki, P.E.D. Morgan, T. Ohji, New uniformly porous $CaZrO_3/MgO$ composites with three-dimensional network structure from natural dolomite. J. Am. Ceram. Soc. 83 (2000) 2091-2093.

[13] Y. Suzuki, N. Kondo, T. Ohji, In situ synthesis and microstructure of porous $CaAl_4O_7$ monolith and $CaAl_4O_7/CaZrO_3$ composite. J. Ceram. Soc. Jpn. 109 (2001) 205-209.

[14] Y. Suzuki, N. Kondo, T. Ohji, P.E.D. Morgan, Uniformly porous composites with 3-D network structure (UPC-3D) for high-temperature filter applications. Int. J. Appl. Ceram. Technol. 1 (2004) 76-85.

[15] Y. Suzuki, M. Tsukatsune, S. Yoshikawa, P.E.D. Morgan, Uniformly porous $Al_2O_3/LaPO_4$

and $Al_2O_3/CePO_4$ composites with narrow pore-size distribution. J. Am. Ceram. Soc. 88 (2005) 3283-3286.

[16] Y Suzuki, P.E.D. Morgan, Meso- and macroporous ceramics by phase separation and reactive sintering methods. MRS Bull. 34 (2009) 587-591.

[17] Y. Suzuki, M. Morimoto, Porous $MgTi_2O_5/MgTiO_3$ composites with narrow pore-size distribution: in situ processing and pore structure analysis. J. Ceram. Soc. Jpn. 118 (2010) 819-822.

[18] Y. Suzuki, M. Morimoto, Uniformly porous $MgTi_2O_5$ with narrow pore-size distribution: in situ processing, microstructure and thermal expansion behavior. J. Ceram. Soc. Jpn. 118 (2010) 1212-1216.

[19] Y. Suzuki, T.S. Suzuki, Y. Shinoda, K. Yoshida, Uniformly porous $MgTi_2O_5$ with narrow pore-size distribution: XAFS study, improved in situ synthesis, and new in situ surface coating. Adv. Eng. Mater. 14 (2012) 1134-1138.

[20] Y. Nakagoshi, Y. Suzuki, Pseudobrookite-type $MgTi_2O_5$ water purification filter with controlled particle morphology. J. Asian. Ceram. Soc. 3 (2015) 334-338.

Table

Table 1 Pore-structure measured by mercury intrusion porosimetry for the porous $MgTi_2O_5$ pellets sintered at 1100°C by using LiF-doped hydromagnesite/TiO_2 mixed powders with various TiO_2 anatase/rutile compositions.

Samples anatase : rutile	V_p [cm^3/g]	S_p [m^2/g]	D_{Mode} [μm]	$D_{Average}$ [μm]	P [%]
(a) 100 : 0	0.357	2.08	0.91	0.88	46.0
(b) 75 : 25	0.438	2.09	1.13	1.08	56.2
(c) 50 : 50	0.457	2.00	1.21	1.18	58.9
(d) 25 : 75	0.511	2.04	1.34	1.29	65.8
(e) 0 : 100	0.495	1.97	1.37	1.29	63.6

V_p: Total pore volume, S_p: Total pore surface area, D_{Mode}: Mode diameter (Peak-top pore diameter), $D_{Average}$: Average pore diameter, P: Porosity
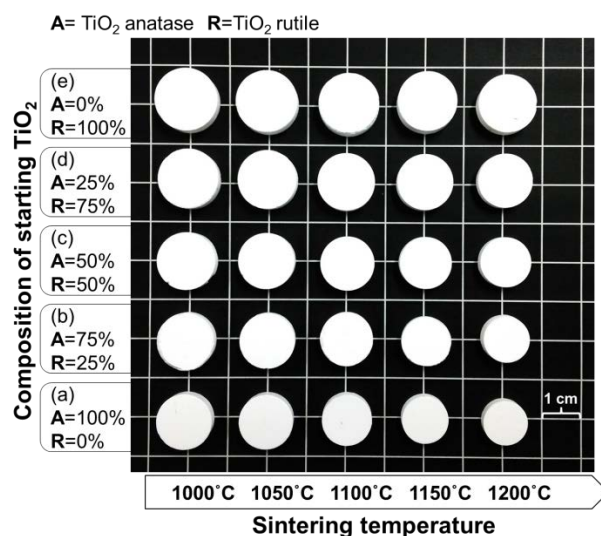
Figure captions

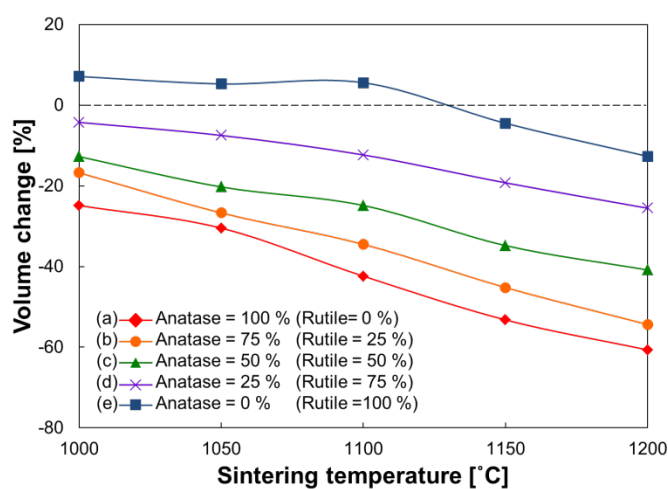**Fig. 1** Appearances of porous $MgTi_2O_5$ pellets by reactive sintering method. Pellet diameter before sintering was 15 mm. Slight volume expansions were observed for the composition (e) sintered at 1000, 1050 and 1100°C.

Fig. 2 Volume change of porous $MgTi_2O_5$ pellets with sintering temperatures. Slight volume expansions were observed for the composition (e) sintered at 1000, 1050 and 1100°C.

Fig. 3 Volume change of porous $MgTi_2O_5$ pellets with changing TiO_2 anatase/rutile composition in the mixed powders. The volume changes are almost proportional to the composition ratio of TiO_2 rutile.

Fig. 4 Pore-size distribution by mercury intrusion porosimetry for $MgTi_2O_5$ pellets sintered at 1100°C by using LiF-doped hydromagnesite/TiO_2 mixed powders with various TiO_2 anatase/rutile compositions: (a) anatase : rutile = 100 : 0, (b) 75 : 25, (c) 50 : 50, (d) 25 : 75 and (e) 0 : 100. All $MgTi_2O_5$ pellets have very narrow pore-size distributions with a diameter of ~1 μm.

Fig. 5 SEM micrographs of porous $MgTi_2O_5$ pellets sintered at 1100°C by using LiF-doped hydromagnesite/TiO_2 mixed powders with various TiO_2 anatase/rutile compositions: (a) anatase : rutile = 100 : 0, (b) 75 : 25, (c) 50 : 50, (d) 25 : 75 and (e) 0 : 100. The $MgTi_2O_5$ pellets became more porous with increasing rutile composition.

Fig. 6 XRD patterns for the $MgTi_2O_5$ powders calcined (without pelletizing) at 1100°C by using LiF-doped hydromagnesite/TiO_2 mixed powders with various TiO_2 anatase/rutile compositions: (a) anatase : rutile = 100 : 0, (b) 75 : 25, (c) 50 : 50, (d) 25 : 75 and (e) 0 : 100. Substantially single-phase $MgTi_2O_5$ powders were obtained. Without pelletizing, very minor $MgTiO_3$ phase (intermediate product) remained.

Fig. 7 High-temperature *in situ* XRD patterns for the selected mixed powders: (a) the hydromagnesite and TiO_2 anatase, and (e) the hydromagnesite and TiO_2 rutile mixed powder both with 0.5 wt.% LiF. Formation temperatures of $MgTiO_3$ and $MgTi_2O_5$ were almost the same in the both mixed powders.

Fig. 8 SEM micrographs of $MgTi_2O_5$ powders calcined at 1100°C by using LiF-doped hydromagnesite/TiO_2 mixed powders with various TiO_2 anatase/rutile compositions: (a) anatase : rutile = 100 : 0, (b) 75 : 25, (c) 50 : 50, (d) 25 : 75 and (e) 0 : 100. Rod-like and coarse particles were obtained only in (a), i.e., by using hydromagnesite/TiO_2 anatase mixed powder with LiF addition, whereas equi-axed and finer particles were obtained for TiO_2 rutile containing mixed powders (b)-(e).

Figures

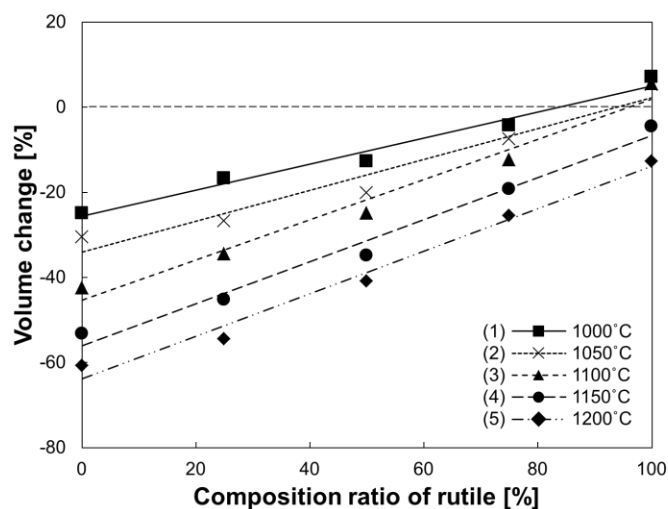**Fig. 1** Appearances of porous $MgTi_2O_5$ pellets by reactive sintering method. Pellet diameter before sintering was 15 mm. Slight volume expansions were observed for the composition (e) sintered at 1000, 1050 and 1100°C.
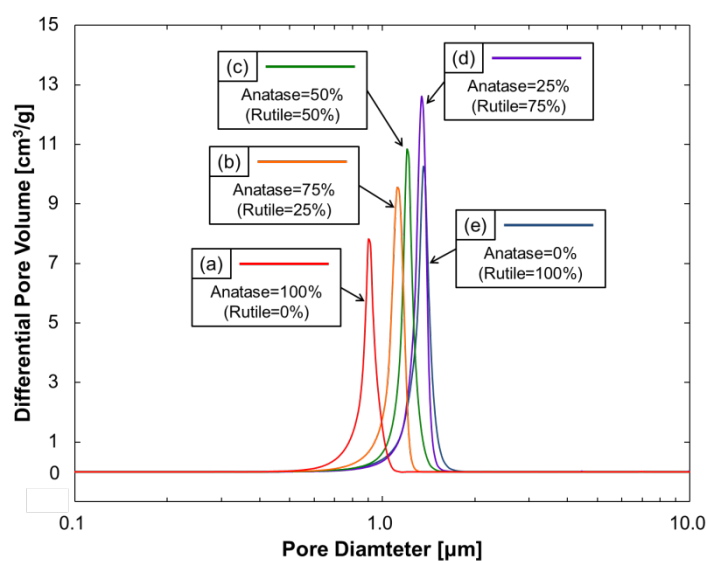

Fig. 2 Volume change of porous $MgTi_2O_5$ pellets with sintering temperatures. Slight volume expansions were observed for the composition (e) sintered at 1000, 1050 and 1100°C.
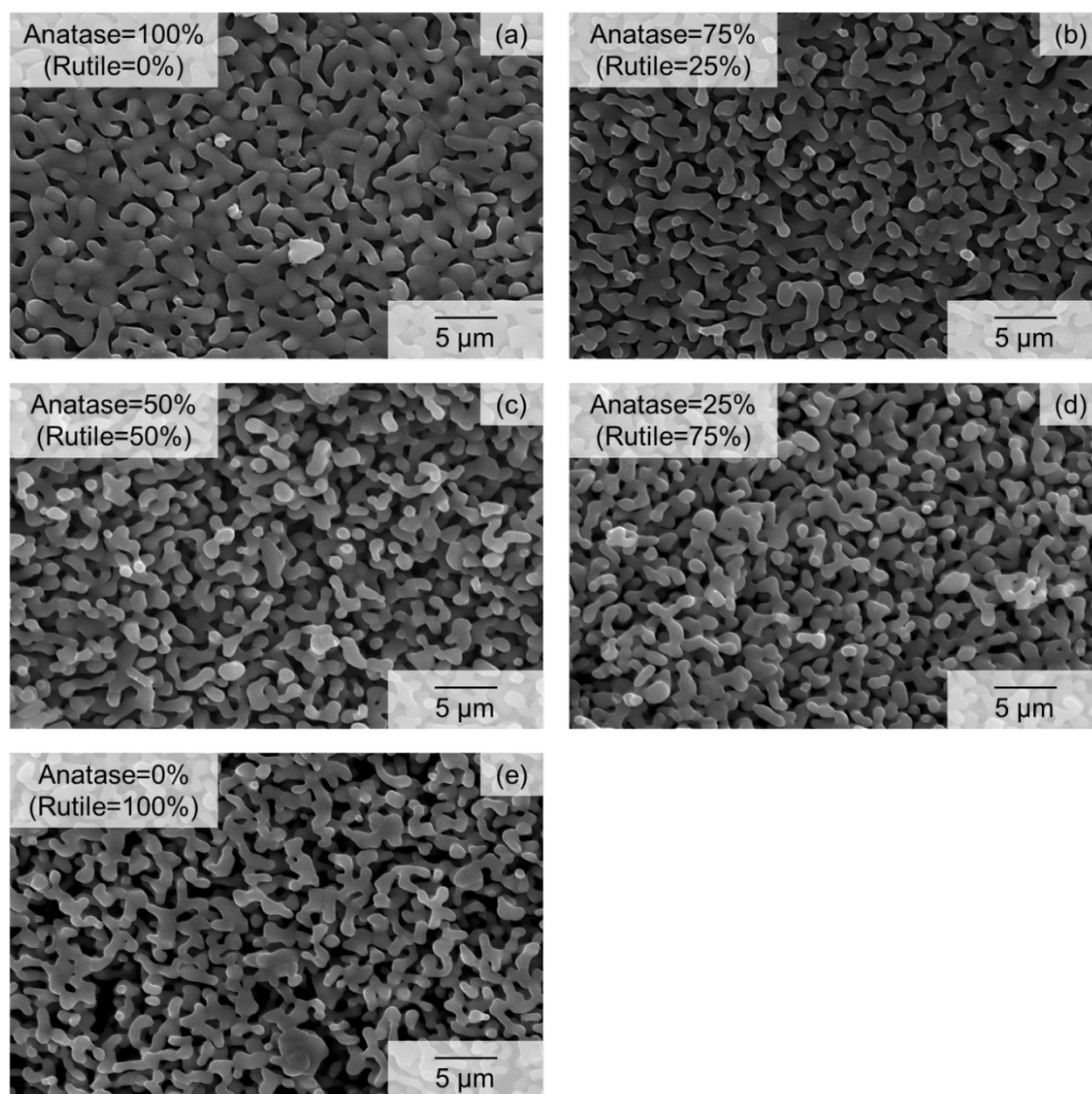
Fig. 3 Volume change of porous $MgTi_2O_5$ pellets with changing TiO_2 anatase/rutile composition in the mixed powders. The volume changes are almost proportional to the composition ratio of TiO_2 rutile.

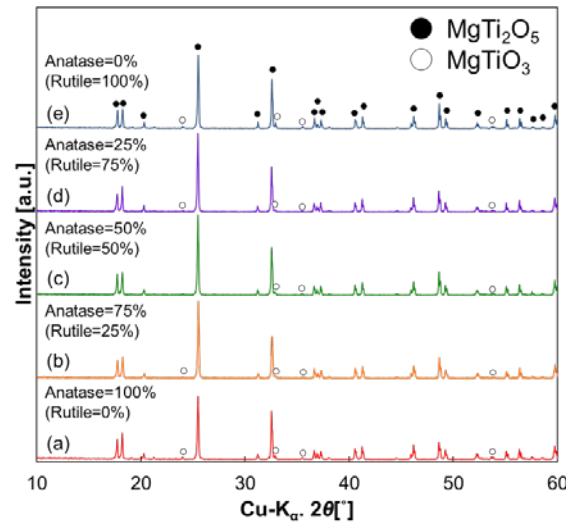**Fig. 4** Pore-size distribution by mercury intrusion porosimetry for $MgTi_2O_5$ pellets sintered at 1100°C by using LiF-doped hydromagnesite/TiO_2 mixed powders with various TiO_2 anatase/rutile compositions: (a) anatase : rutile = 100 : 0, (b) 75 : 25, (c) 50 : 50, (d) 25 : 75 and (e) 0 : 100. All $MgTi_2O_5$ pellets have very narrow pore-size distributions with a diameter of ~1 μm.
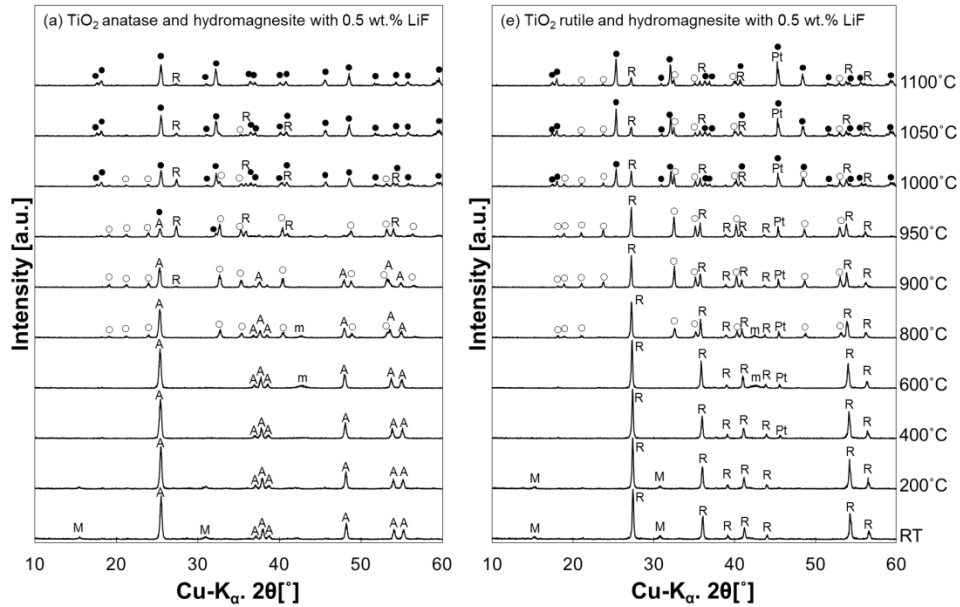
Fig. 5 SEM micrographs of porous $MgTi_2O_5$ pellets sintered at 1100°C by using LiF-doped hydromagnesite/TiO_2 mixed powders with various TiO_2 anatase/rutile compositions: (a) anatase : rutile = 100 : 0, (b) 75 : 25, (c) 50 : 50, (d) 25 : 75 and (e) 0 : 100. The $MgTi_2O_5$ pellets became more porous with increasing rutile composition.
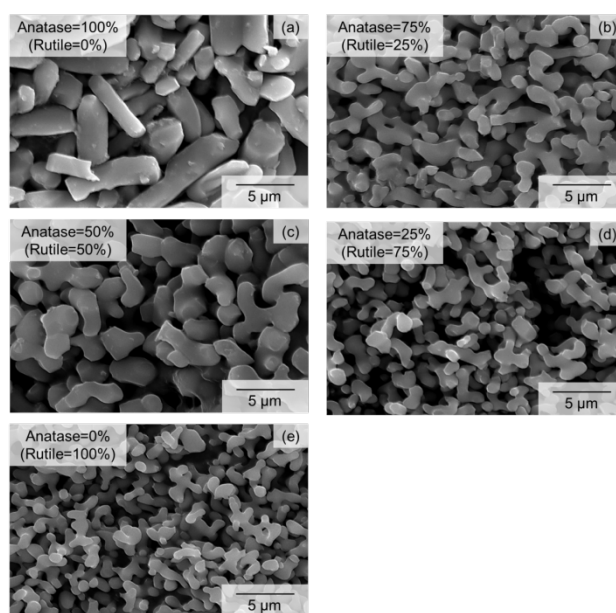
Fig. 6 XRD patterns for the MgTi₂O₅ powders calcined (without pelletizing) at 1100°C by using LiF-doped hydromagnesite/TiO₂ mixed powders with various TiO₂ anatase/rutile compositions: (a) anatase : rutile = 100 : 0, (b) 75 : 25, (c) 50 : 50, (d) 25 : 75 and (e) 0 : 100. Substantially single-phase MgTi₂O₅ powders were obtained. Without pelletizing, very minor MgTiO₃ phase (intermediate product) remained.

Fig. 7 High-temperature *in situ* XRD patterns for the selected mixed powders: (a) the hydromagnesite and TiO₂ anatase, and (e) the hydromagnesite and TiO₂ rutile mixed powder both with 0.5 wt.% LiF. Formation temperatures of MgTiO₃ and MgTi₂O₅ were almost the same in the both mixed powders.

**Fig. 8** SEM micrographs of $MgTi_2O_5$ powders calcined at 1100°C by using LiF-doped hydromagnesite/TiO_2 mixed powders with various TiO_2 anatase/rutile compositions: (a) anatase : rutile = 100 : 0, (b) 75 : 25, (c) 50 : 50, (d) 25 : 75 and (e) 0 : 100. Rod-like and coarse particles were obtained only in (a), i.e., by using hydromagnesite/TiO_2 anatase mixed powder with LiF addition, whereas equi-axed and finer particles were obtained for TiO_2 rutile containing mixed powders (b)-(e).

Supporting information

The particle-size distribution and the average particle-size of the mixed powders after sieving (through a 150-mesh screen) were measured by the dynamic light scattering method (FDLS-3000, Otsuka Electronics, Osaka, Japan) as shown in **Figure S1** and **Table S1**. Particle size distributions were somewhat larger for the anatase/rutile mixed compositions, but all mixed powders had almost the same average particle-sizes (about 480-580 nm).
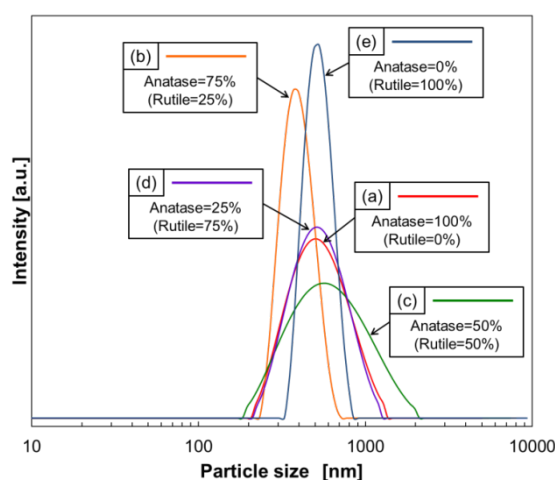
Fig. S1 Particle-size distributions by dynamic light scattering for the mixed powders after sieving: (a) anatase : rutile = 100 : 0, (b) 75 : 25, (c) 50 : 50, (d) 25 : 75 and (e) 0 : 100.

Table S1 Average particle size ($D_{Average}$) and mode particle size (D_{Mode}) of the mixed powders measured by dynamic light scattering. All powders have almost same average particle size: 480~580 nm.

Mixed powders anatase : rutile	$D_{Average}$ [nm]	D_{Mode} [nm]
(a) 100 : 0	486.5	498.6
(b) 75 : 25	509.5	399.1
(c) 50 : 50	533.0	563.3
(d) 25 : 75	489.6	501.7
(e) 0 : 100	575.5	527.0